Lithos 300–301 (2018) 250–260

Contents lists available at ScienceDirect

Lithos

journal homepage: www.elsevier.com/locate/lithos

Geochronological and geochemical constraints on the origin of the Yunzhug ophiolite in the Shiquanhe–Yunzhug–Namu Tso ophiolite belt, Lhasa Terrane, Tibetan Plateau

Yun-Chuan Zeng [a], Ji-Feng Xu [a,b,*], Jian-Lin Chen [b], Bao-Di Wang [c], Zhi-Qiang Kang [d], Feng Huang [a]

[a] State Key Laboratory of Geological Processes and Mineral Resources, School of Earth Science and Resources, China University of Geosciences, Beijing 100083, China
[b] State Key Laboratory of Isotope Geochemistry, Guangzhou Institute of Geochemistry, Chinese Academy of Sciences, Guangzhou 510640, China
[c] Chengdu Institute of Geology and Mineral Resources, Chengdu 610081, China
[d] School of Earth Science and Guangxi Key Laboratory of Hidden Metallic Ore Deposits Exploration, Guilin University of Technology, Guilin 541004, China

ARTICLE INFO

Article history:
Received 6 September 2017
Accepted 23 November 2017
Available online 27 November 2017

Keywords:
Ophiolite
Lhasa Terrane
Tectonic evolution
Embryonic ocean
MORB

ABSTRACT

The formation of the Shiquanhe–Yunzhug–Namu Tso ophiolite mélange zone (SNMZ) within the Lhasa Terrane, Tibetan Plateau, is key to understanding the Mesozoic tectonic evolution of this terrane, which remains controversial. We show that the Yunzhug ophiolite in the central segment of the SNMZ formed at ~150 Ma, based on U–Pb dating of zircons from a gabbroic sample in a well-developed sheeted dike complex. Geochemically, these mafic rocks are dominated by E-MORB-type compositions, along with minor amounts of rocks with P-MORB-type compositions. The samples also exhibit high $\varepsilon_{Nd}(t)$ values and lack negative Nb and Ta anomalies. Data for all the samples plot within the MORB array on a Th/Yb–Nb/Yb diagram. Therefore, these mafic rocks most likely formed in either a slow spreading oceanic setting or an embryonic ocean, and not in a back-arc basin as has been previously assumed. Taking into account the regional geology, we propose that the Yunzhug ophiolite is part of a distinct ophiolitic belt and represents material formed in an embryonic ocean within the Lhasa Terrane, which provides new insights into the Jurassic tectonic evolution of the Lhasa Terrane.

1. Introduction

The Himalayan–Tibetan Plateau was created by the collision of the Indian and Eurasian plates, and has been the subject of many studies of collisional processes (Fig. 1a) (Chung et al., 2005; Ji et al., 2016; Yin and Harrison, 2000). However, to better understand its collisional history, it is necessary to reconstruct the pre-collisional geological evolution of the Tibetan Plateau, especially the Mesozoic evolution of the Lhasa Terrane, which remains debated (e.g., Coulon et al., 1986; Yin and Harrison, 2000; Kapp et al., 2003, 2007; Zhu et al., 2011; Zhang et al., 2011, 2012; K. J. Zhang et al., 2014; Z. M. Zhang et al., 2014; Zeng et al., 2016, 2017; Li et al., 2017). One point of debate is how an ophiolitic belt such as the Shiquanhe–Yunzhug–Namu Tso ophiolite mélange zone (SNMZ) could form within the Lhasa Terrane (Fig. 1b). As such, any valid model for the Mesozoic tectonic evolution of the terrane needs to explain this ophiolite occurrence. It remains unclear whether the SNMZ represents: (a) a discrete remnant of an independent ophiolitic belt (e.g., Pan et al., 2012; Xu et al., 2014a; Zhu et al., 2013); (b) a southward-directed nappe of the Bangong–Nujiang ophiolites (e.g., Baxter et al., 2009; Girardeau et al., 1985; Kapp et al., 2003; Y. X. Zhang et al., 2007); or (c) an intra-oceanic system within the Bangong–Nujiang Ocean (e.g., Matte et al., 1996; K. J. Zhang et al., 2014). However, given the currently limited geochronological and geochemical evidence available, the tectonic setting for the formation of the SNMZ remains uncertain (Xu et al., 2014a; Zhu et al., 2013). The Yunzhug ophiolite is found in the central segment of the SNMZ (Fig. 1b), and preserves a nearly complete ophiolite sequence (Fig. 2). Therefore, it provides an ideal opportunity to clarify the tectonic environment of its formation and the origin of the SNMZ. However, previous studies of this ophiolite have provided either discordant zircon U–Pb ages for the sheeted dikes or K–Ar ages for the pillow basalts (Wang et al., 2005; Zhu, 2004), and none of these ages are reliable due to either Pb loss or alteration. Our new zircon U–Pb ages for the sheeted dike complex presented herein reveal a Late Jurassic age (ca. 150 Ma) for these rocks. Moreover, these mafic rocks exhibit typical mid-ocean ridge basalt (MORB)-like geochemical characteristics without subduction signatures, which are inconsistent with the conventionally accepted back-arc basin model for the formation of this ophiolitic belt (e.g., Xu et al., 2014a; Zhu et al., 2011, 2013). Therefore, the Yunzhug ophiolite has the potential to provide new insights into the Jurassic tectonic evolution of the Lhasa Terrane.

* Corresponding author at: 29 Xueyuan Road, Haidian District, Beijing 100083, China.
E-mail address: jifengxu@gig.ac.cn (J.-F. Xu).

https://doi.org/10.1016/j.lithos.2017.11.025
0024-4937/

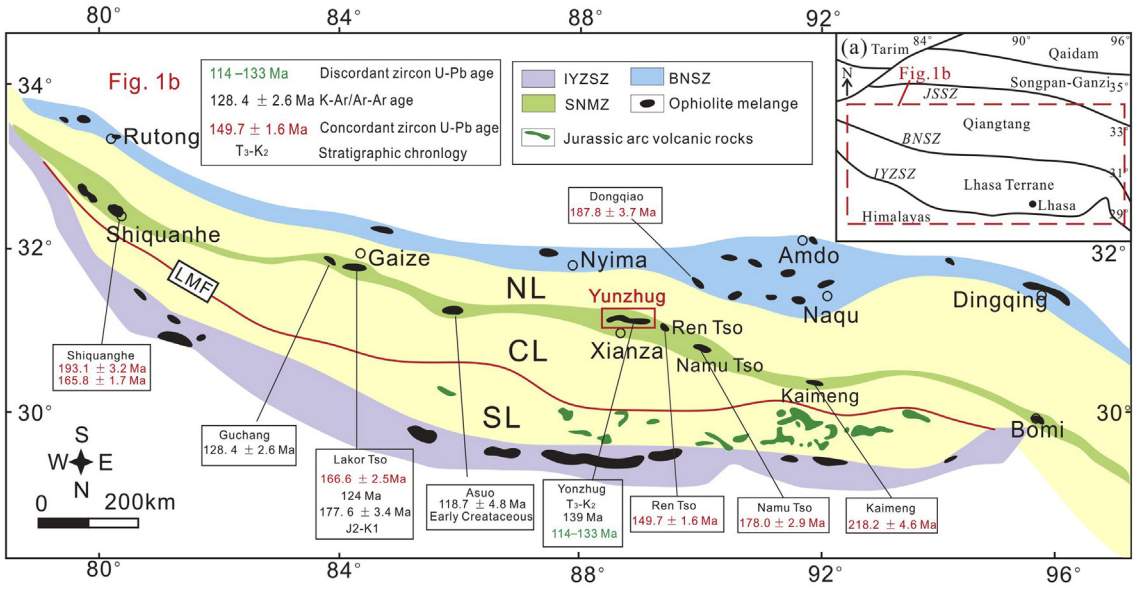

Fig. 1. (a) Simplified geological map of the Tibetan Plateau and (b) general outline of the three ophiolitic belts on the margins and in the interior of the Lhasa Terrane (modified from Xu et al., 2014a; Yin and Harrison, 2000; Zhu et al., 2011). Abbreviations: IYZSZ = Indus–Yarlung Zangbo Suture Zone; BNSZ = Bangong–Nujiang Suture Zone; JSSZ = Jinsha Suture Zone; SNMZ = Shiquanhe–Yunzhug–Namu Tso ophiolite mélange zone; LMF = Luobadui–Milashan Fault; SL = southern Lhasa subterrane; CL = central Lhasa subterrane; NL = northern Lhasa subterrane. The age of the Dongqiao Ophiolite in the BNSZ is from Liu et al. (2016), and those for the ophiolites of the SNMZ are from Zhu (2004), Y. X. Zhang et al. (2007), Zheng et al. (2006), Wang et al. (2008), Zhong et al. (2015), and He et al. (2006).

2. Geological setting and field occurrence

2.1. Regional geology

The Himalayan–Tibetan Plateau comprises four parts, which from north to south are the Songpan–Ganzi, Qiangtang, Lhasa, and Himalaya terranes, separated by three suture zones (Fig. 1a). The Lhasa Terrane is adjacent to the Qiangtang and Himalayan terranes, and is bounded by the Bangong–Nujiang Suture Zone (BNSZ) to the north and the Indus–Yarlung–Zangbo Suture Zone (IYZSZ) to the south (Yin and Harrison, 2000; Zhu et al., 2013; Wu et al., 2017) (Fig. 1a). Zircon U–Pb dating of mafic rocks has revealed that the ophiolites from these two suture zones mainly formed during Early–Middle Jurassic and Early Cretaceous, respectively (Liu et al., 2016; Wang et al., 2016; Xu et al., 2014a). Based on the zircon Hf isotopic compositions of late Mesozoic to early Tertiary igneous rocks, the terrane can be further subdivided into the southern, central, and northern subterranes (Fig. 1b) (Zhu et al., 2011). The main units exposed in the northern Lhasa subterrane are Middle Triassic to Cretaceous sedimentary rocks and Early Cretaceous igneous rocks. The southern Lhasa subterrane is dominated by a Cretaceous–Tertiary batholith and the Paleogene Linzizong volcanic rocks (Ji et al., 2009; Zhu et al., 2013), along with minor Early Jurassic–Cretaceous volcanic–sedimentary rocks (e.g., Kang et al., 2014; Zhu et al., 2013). The igneous rocks from these two subterranes provide evidence for the existence of juvenile continental crust (Ji et al., 2009; Zhu et al., 2011). In contrast, the central Lhasa subterrane comprises Proterozoic–Archean basement that is mainly covered by Paleozoic and Upper Jurassic–Lower Cretaceous sedimentary units that contain abundant volcanic rocks.

The SNMZ is an ophiolitic belt that extends intermittently for >2000 km, from Shiquanhe in the west to Bomi in the east (Fig. 1b). In general, the ophiolite sequences in this belt are strongly dismembered, but assemblages of peridotite, gabbro, diabase, and pillow basalt interbedded with radiolarite-bearing siliceous rocks crop out in close proximity in each ophiolite segment (Baxter et al., 2009; Kapp et al., 2003; Wang et al., 2008; Xu et al., 2014a), thus meeting the criteria for a dismembered ophiolite (Robertson, 2002). The ophiolite subunits in each segment are all in fault contact with Paleozoic to Early Cretaceous sedimentary rocks, and share consistent radiolarite ages ranging from Middle Jurassic to Early Cretaceous. A relatively complete ophiolite sequence is preserved in the Yunzhug (Fig. 2) and Lakor Tso areas (Yuan et al., 2015).

The sedimentary strata in the Yunzhug area include the Neoproterozoic Nianqingtanggula Formation, Paleozoic continental shelf strata, the Upper Jurassic–Lower Cretaceous Rila Formation, and Lower Cretaceous volcanic–sedimentary rocks (Fig. 2) (Volkmer et al., 2014; Xu et al., 2014a; Zhang et al., 2011). The Yunzhug ophiolite preserves a nearly complete ophiolite sequence of peridotites, cumulates, a sheeted dike complex, pillow basalts, and siliceous rocks (Fig. 2). In general, the dismembered ophiolite subunits are in faulted contact with Paleozoic sedimentary rocks (Figs. 2a and 3a), apart from the peridotite, which is overlain by the Rila Formation across a nonconformity (Fig. 3b) (Qu et al., 2003). These structural relationships may be related to ophiolite emplacement. Fracture zones and/or mylonites are observed in the contact zone between the ophiolite subunits and Paleozoic sedimentary rocks. Peridotites and cumulate rocks are mainly found on the southwestern bank of Guomang Tso. The peridotites are dominantly harzburgite, along with minor dunite and lherzolite with enclosed podiform chromite, which are all mostly serpentinized (Fig. 3a–c). The cumulate rocks include gabbros and leucogabbros that are in tectonic contact with the mantle peridotites. The gabbros exhibit typical cumulate layering structures (Fig. 3d). The leucogabbros occur as dikes within the layered gabbros and lack any obvious signs of chilled margins (Fig. 3c), which implies multi-phase crystal fractionation and accumulation. To the east of the cumulate rocks, peridotites are again found, but not as abundantly as to the west. These peridotites are in tectonic contact with a well-developed sheeted dike complex on the southeastern bank of Guomang Tso. The sheeted dike complex consists of sub-parallel diabasic and gabbroic dikes (Fig. 3e–f). Individual dike widths vary from 8 to 150 cm, and each may exhibit one or two (the majority) chilled margins. Farther east, the sheeted dike complex shows a gradual transition into (or locally intrudes) a series of basalts (Fig. 3e), which include pillow (mostly) and brecciated basalts. The pillow basalts are intercalated with layers of red siliceous rocks (10–50 cm thick) (Fig. 3d). The radiolarites in the siliceous rocks contain a Middle Jurassic to Early Cretaceous assemblage (Wang et al., 2005).

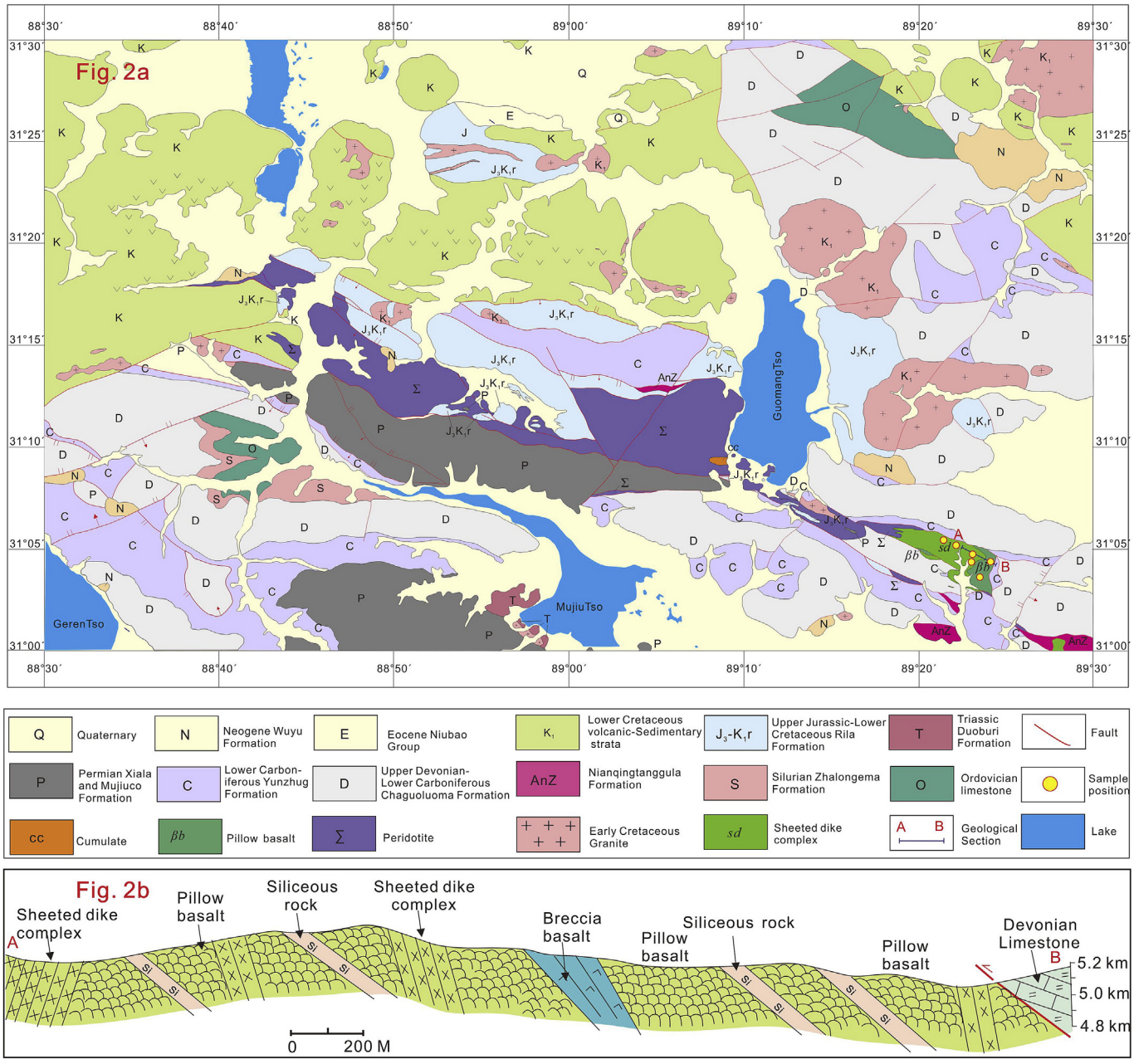

Fig. 2. Geological map of the Yunzhug area.
(From Wang et al., 2005).

2.2. Sample descriptions

The mafic dikes and pillow basalts in the study area have undergone low-grade metamorphism. The basalts are porphyritic, containing 10%–15% phenocrysts that are mainly altered plagioclase, clinopyroxene, and minor olivine (Fig. 4a). The matrix includes plagioclase, clinopyroxene, spinel, and interstitial Fe–Ti oxides. Chloritization and epidotization are widely developed in the gabbroic dikes, which are medium- to coarse-grained and consist of euhedral plagioclase, anhedral clinopyroxene (partly replaced by actinolite), and accessory minerals such as magnetite and zircon (Fig. 4b–c). In the diabasic dikes, anhedral clinopyroxene crystals enclose euhedral plagioclase crystals, representing a typical ophitic texture (Fig. 4d). Accessory minerals include magnetite, zircon, and apatite. Secondary chlorite and epidote converted from clinopyroxene and plagioclase during rodingitization, are present in minor but variable amounts.

3. Analytical methods and results

Details of our analytical methods, including zircon U–Pb dating, whole-rock major and trace element analyses, and whole-rock Sr–Nd isotopic analyses, are given in Supplementary Text S1.

3.1. Zircon U–Pb geochronology

One gabbroic sample from the sheeted dike complex was used for zircon U–Pb geochronology. Ten spots on zircons from sample 13MB-01 yielded concordant $^{206}Pb/^{238}U$ ages of 143.5 ± 6.1 to 160.8 ± 5.5 Ma, with a weighted mean age of 150.5 ± 3.6 Ma (Table S1) (Fig. 5a). All the analyzed zircons are either long, euhedral, and prismatic crystals, or broken prisms, with lengths of ~45 to 150 μm. Internally, the zircon crystals are quite homogeneous with weak, broad zoning without complex internal structures in cathodoluminescence (CL) images

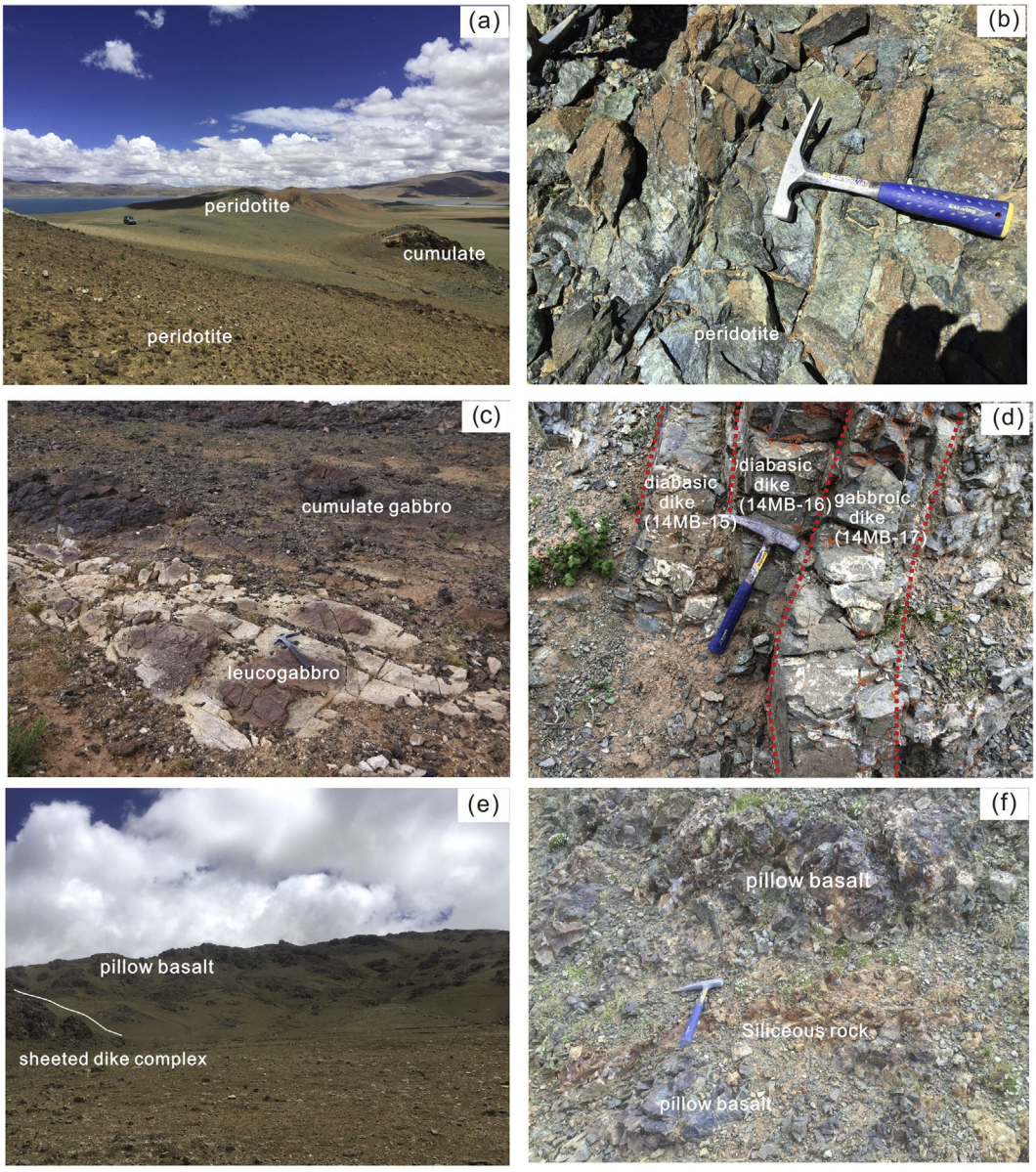

Fig. 3. Field photographs of the ophiolitic members in the Yunzhug area: (a) peridotite and cumulates on the west bank of Guomang Tso; (b) peridotite; (c) layered gabbros and leucogabbros; (d) sheeted dike complex; (e) sheeted dike complex and pillow basalt; and (f) pillow basalt with layered siliceous rocks.

(Fig. 5b), which is typical of zircons formed in gabbroic magmas (Corfu et al., 2003). In addition, no overgrowths, mineral or fluid inclusions, or metamictization was observed in the analyzed zircons, which suggest that the zircons were not affected by post-magmatic processes (Fig. 5b). The high Th/U ratios (≥0.5) (Table S2), strongly depleted light rare earth element (LREE) patterns, and negative Eu anomalies (Fig. 5c) in the zircons further demonstrate their magmatic origin (Corfu et al., 2003; Hoskin and Black, 2000). Moreover, the zircon Y, U, and Yb contents are comparable with those of zircons from oceanic crust (Fig. 5d). In summary, our new age data indicate formation of the dikes at ca. 150 Ma.

3.2. Whole-rock major and trace element data

The mafic rocks (sheeted dikes and pillow basalts) have undergone low-degree of alteration, as reflected by their LOI values (Table S3) and petrography (Fig. 4). As such, the major element data for the Yunzhug mafic rocks have been recalculated on an anhydrous basis. On a Zr/TiO_2 vs. Nb/Y diagram (Fig. 6a), data for all the Yunzhug mafic rocks plot in the basalt field, and on a Ti/1000 vs. V diagram (Fig. 6b) they plot within the MORB field. Based on their geochemistry, the Yunzhug mafic rocks can be further divided into two groups: E-MORB-type (enriched MORB) and P-MORB-type (plume-type MORB) (Saccani et al., 2013). The E-MORB-type rocks are subalkaline and have flat or slightly LREE-enriched chondrite-normalized REE patterns (Fig. 7a), and moderate $(La/Sm)_N$ (N = normalized to primitive mantle values of Sun and McDonough, 1989) and Zr/Nb ratios (Table S3). Data for these rocks consistently plot in the E-MORB compositional field (Fig. 8), and their Th/Yb and Nb/Yb ratios are similar to typical E-MORB values (Fig. 9). The P-MORB-type rocks are alkaline pillow basalts (Fig. 6a) that have higher Nb and Ta contents, and higher $(La/Sm)_N$ but lower Zr/Nb ratios than the E-MORB-type rocks (Table S3). In addition, data for the P-MORB-type rocks plot in the within-plate basalt (WPB) field and in the transitional area between the P-MORB and alkaline basalt fields (Fig. 8). The P-MORB-type rocks have higher Th/Yb and Nb/Yb ratios than the E-MORB-type rocks (Fig. 9).

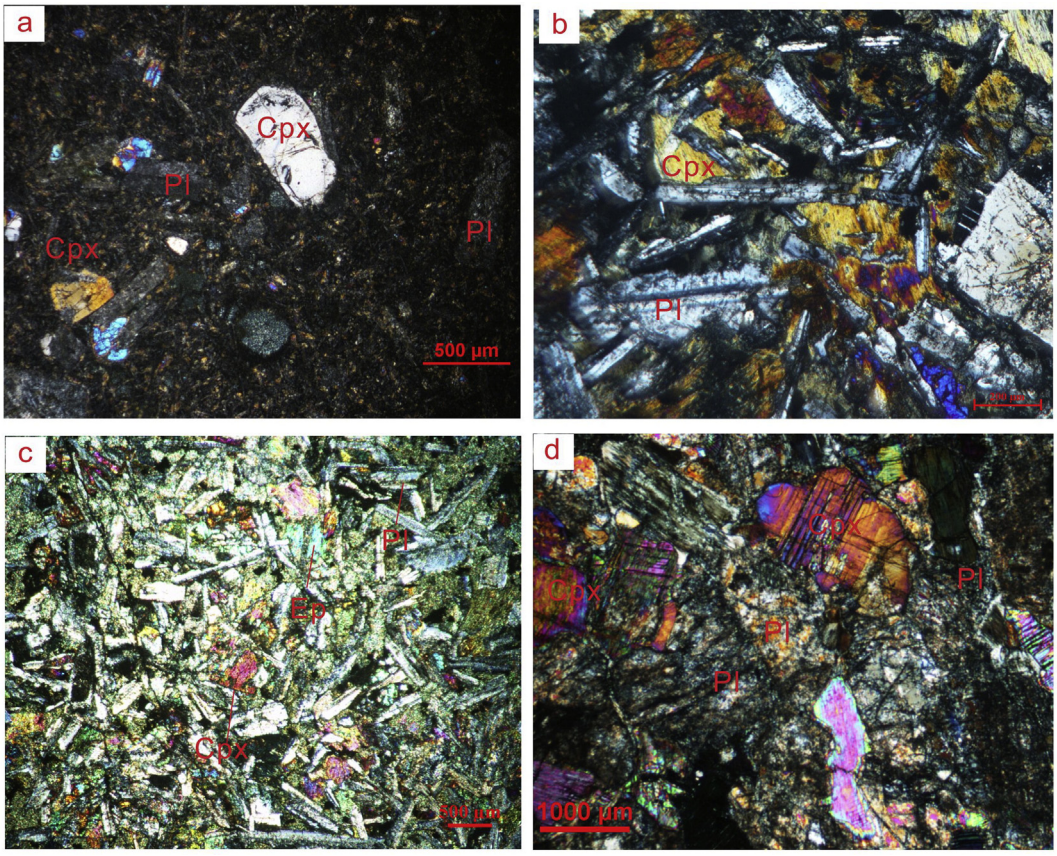

Fig. 4. Microphotograph for the Yunzhug ophiolite subunits: (a) pillow basalts; (b–c) diabasic dike; (d) gabbroic dike. Abbreviations: Ep = Epidote; Cpx = clinopyroxene; Pl = plagioclase; Ol = olivine.

3.3. Sr–Nd isotopes

The E-MORB-type rocks have $(^{87}Sr/^{86}Sr)_i$ values of 0.703586 to 0.705206 and $(^{143}Nd/^{144}Nd)_i$ values of 0.512787 to 0.512891 ($\varepsilon_{Nd}(t) = +6.72$ to $+8.74$) (Table S4). The P-MORB-type rocks have $(^{87}Sr/^{86}Sr)_i$ values of 0.704496 to 0.705527 and $(^{143}Nd/^{144}Nd)_i$ values of 0.512756 to 0.512786 ($\varepsilon_{Nd}(t) = +6.09$ to $+6.68$). The high $(^{87}Sr/^{86}Sr)_i$ values of both groups of rock are due to alteration, as also indicated by a positive correlation between $(^{87}Sr/^{86}Sr)_i$ and LOI values (not shown).

4. Ages of the ophiolites in the SNMZ

The formation age of the SNMZ remains controversial, and the debate focuses on whether the SNMZ formed in the late Early Cretaceous or earlier (i.e., Late Triassic or Middle–Late Jurassic) (Pan et al., 2012; Xu et al., 2014a; Yuan et al., 2015; Y. X. Zhang et al., 2007; Zhong et al., 2015; Zhu et al., 2013) (Fig. 1b). Notably, the previously obtained Early Cretaceous ages were derived from whole-rock K–Ar dating or discordant zircon U–Pb results (Fig. 1b). The whole-rock K–Ar ages are unreliable because the crustal rocks in the ophiolites have generally undergone severe alteration and metamorphism, and the discordant zircon U–Pb ages are also unreliable due to Pb loss during metamorphism (Yuan et al., 2004, 2008). Although the available concordant zircon U–Pb ages range from Late Triassic to Middle–Late Jurassic (Fig. 1b), zircons from the Kaimeng troctolites (218.2 ± 4.6 Ma) and the Shiquanhe olivine pyroxenites (193.1 ± 3.2 Ma) exhibit heterogeneous internal textures and numerous narrow oscillatory zones in cathodoluminescence images (He et al., 2006; Zheng et al., 2006), whereas zircons from the basaltic rocks are generally homogeneous with weak, broad zoning without complex internal structures (e.g., Corfu et al., 2003; Hoskin, 2000). The dated samples from the two previous studies are Si-undersaturated and have low Th (<0.07 ppm) and U (<0.03 ppm) contents, which are inconsistent with the extremely high Th and U contents of the analyzed zircons (up to 1128 and 1879 ppm, respectively) (e.g., Grimes et al., 2015). Despite the concordance of the zircon U–Pb age (178 ± 2.9 Ma) obtained for the Namu Tso metagabbro, no geochemical data for this metagabbro have been reported (Zhong et al., 2015). Moreover, the analyzed zircons show distinct core–rim structures and have lower $\varepsilon_{Hf}(t)$ values than those from the Ren Tso gabbros (Zhong et al., 2015). For the Yunzhug ophiolite, Wang et al. (2005) and Zhu (2004) reported a K–Ar age (139 Ma) for pillow basalts and discordant zircon U–Pb ages (114–133 Ma) for gabbroic dikes. As discussed above, these results require further scrutiny. It must be noted that the zircons from the two MORB-type dikes that we analyzed show features that are typical of oceanic-type zircons (Fig. 5b). Therefore, we propose that the zircon U–Pb ages obtained from the Shiquanhe diorite (165.8 ± 1.7 Ma), Lagkor Tso plagiogranite (166.6 ± 2.5 Ma), Ren Tso gabbro (149.7 ± 1.6 Ma) (Fig. 1b), and Yunzhug gabbroic dike (150.5 ± 3.6 Ma), along with supporting geochemical data, provide the only reliable currently available sources of information to constrain the formation, age, and tectonic setting of the SNMZ. Our new zircon U–Pb ages are also consistent with the ages of radiolarites (Middle Jurassic–Early Cretaceous) in the siliceous rocks of this belt (Qu et al., 2003; Zheng et al., 2006).

5. Petrogenesis of the mafic rocks

Given the lack of negative Nb–Ta anomalies and high $\varepsilon_{Nd}(t)$ values of the Yunzhug mafic rocks (Figs. 7 and 10), crustal contamination is negligible in the petrogenesis of these rocks. Although the E-MORB- and P-MORB-type rocks have different $Mg^{\#}$, and MgO, Cr, and Ni

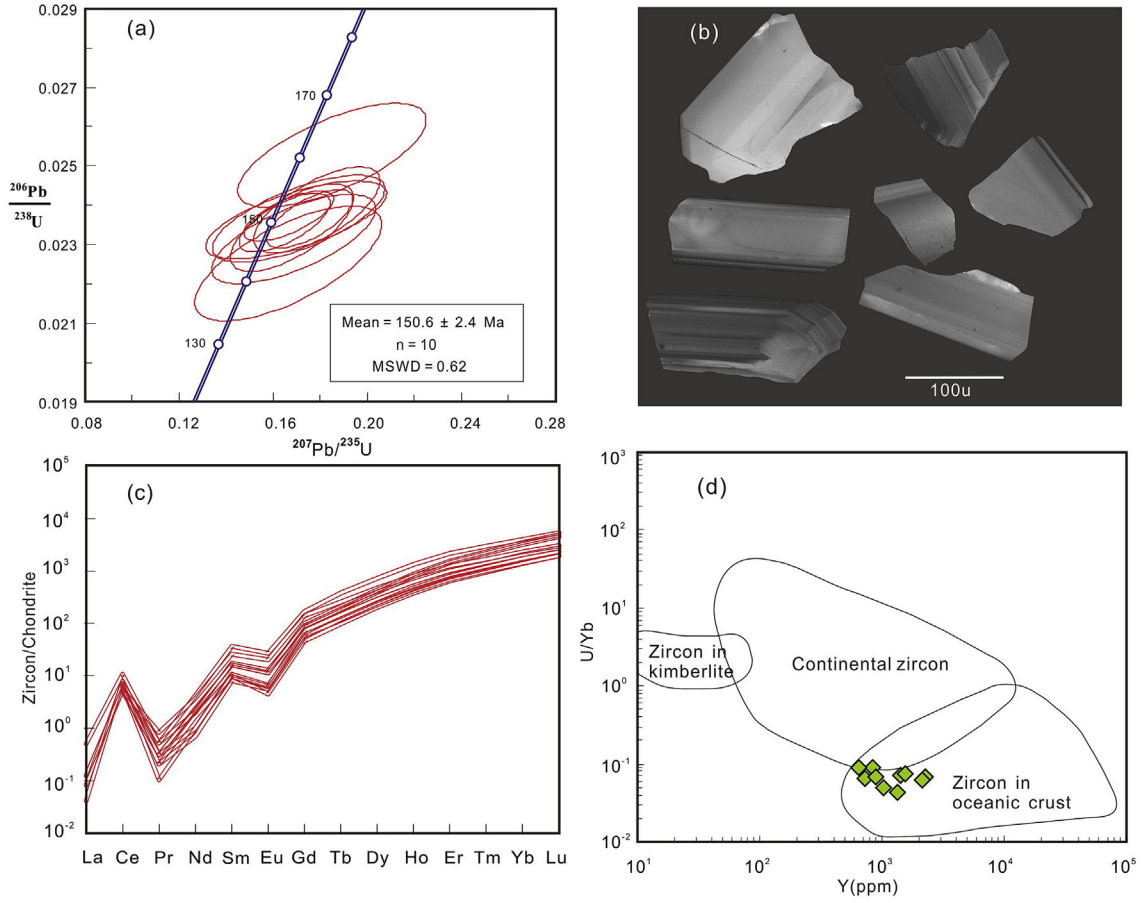

Fig. 5. (a) U–Pb concordia diagrams for zircons in the gabbroic dikes of the Yunzhug ophiolite. (b) Representative cathodoluminescence images, (c) chondrite-normalized REEs pattern (Sun and McDonough, 1989) and (d) U/Yb-Y plot (Grimes et al., 2007) for zircons in the gabbroic dikes of the Yunzhug ophiolite. Data for LakorTso ophiolite are from Yuan et al. (2015) and for RenTso ophiolite are from Zhong et al. (2015).

contents, reflecting different extents of fractional crystallization, their distinctly different Zr/Nb ratios and $\varepsilon_{Nd}(t)$ values cannot be attributed to fractional crystallization or partial melting (Fig. 10; Table S3). This indicates that the E-MORB- and P-MORB-type rocks were derived from heterogeneous sources. Similar to E-MORB-type rocks worldwide, the high $\varepsilon_{Nd}(t)$ and lower $^{147}Sm/^{144}Nd$ values than depleted mantle (0.215; Goldstein et al., 1984) indicate that the source of the MORB-type rocks in the study area was recently enriched. The occurrence of P-MORB-type rocks, along with within-plate enrichment trends (Fig. 8) and negative correlations between Nb/Yb ratios and $\varepsilon_{Nd}(t)$ values (Fig. 10b) for the two groups of rocks indicate the contribution of ocean island basalt (OIB)-like components (e.g., Leat et al., 2000). These OIB components may be related to a mantle plume, recycled oceanic lithosphere, delaminated continental crust, or enriched lithospheric

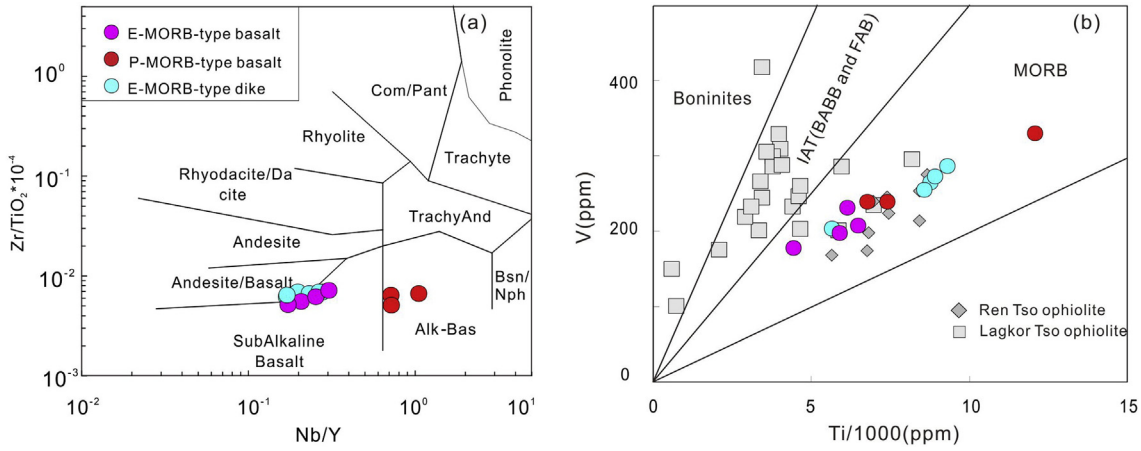

Fig. 6. Nb/Y versus Zr/TiO_2 (after Winchester and Floyd, 1977) and Ti/1000 versus V (after Shervais, 1982) diagrams. Abbreviations: FAB = fore-arc basalt; BABB = back-arc basin basalt; IAT = island arc tholeiite.

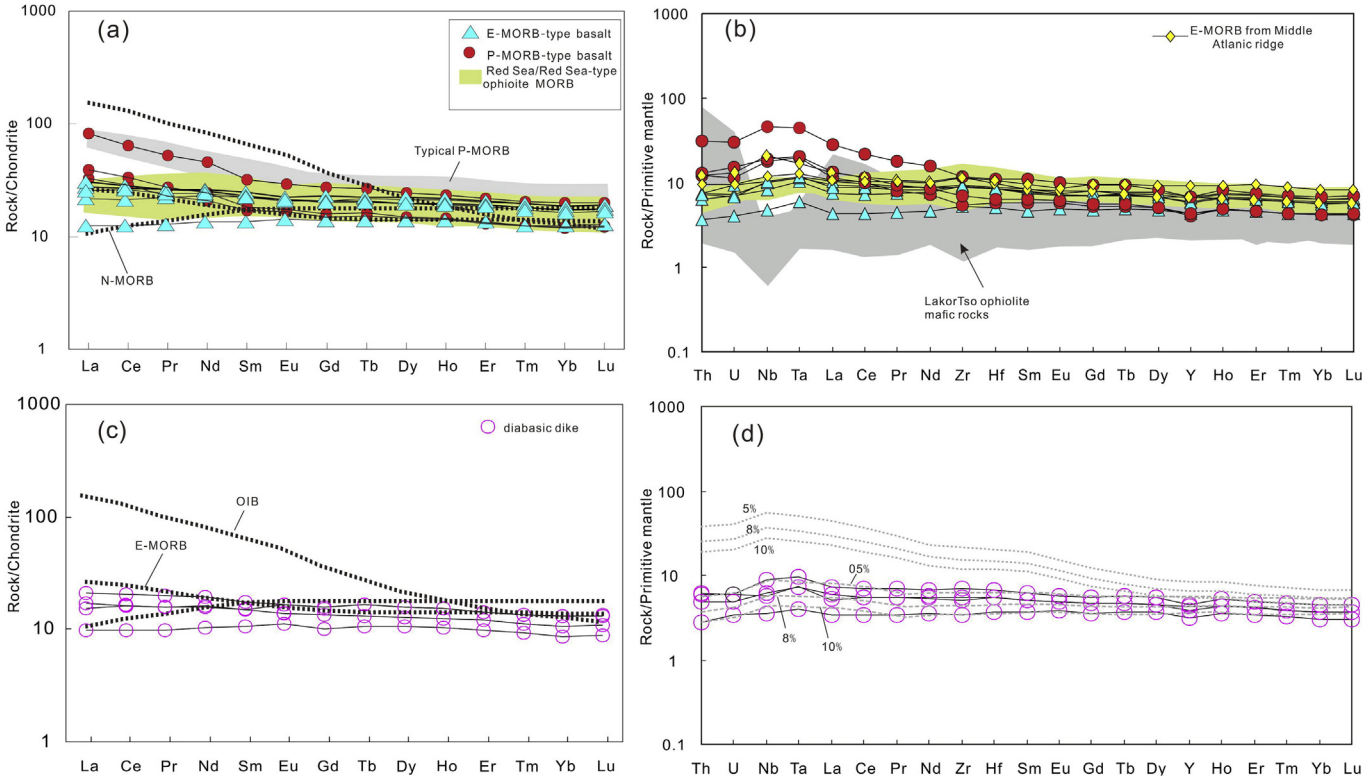

Fig. 7. Chondrite-normalized REE and primitive-mantle-normalized multi-element plots. P-MORB values are from Saccani et al. (2013), and the primitive mantle, chondrite, N-MORB, E-MORB, and OIB values are from Sun and McDonough (1989). Fractional partial melt modeling, partition coefficients, depleted mantle, and the possible compositions of OIB-like enriched materials are from Donnelly et al. (2004) and Ulrich et al. (2012). The source mineral proportions are 18% clinopyroxene, 30% orthopyroxene, and 52% olivine in the source, and 75% clinopyroxene, −10% orthopyroxene, and 35% olivine in the melt. The E-MORB- and P-MORB-type rocks can be generated by 5%–10% melting with enrichment degrees of ~1% and ~5%, respectively. Data for Red Sea MORB are from Petrini et al. (1988) and Haase et al. (2000), and MAR–SWIR values are from Ulrich et al. (2012). Data for LakorTso ophiolite are from Yuan et al. (2015) and for RenTso ophiolite are from Zhong et al. (2015).

mantle veins (Dilek and Furnes, 2011; Donnelly et al., 2004; Rehka and Hofmann, 1997; Saccani et al., 2013; Waters et al., 2011). Accurately distinguishing the origin of the OIB-like component is difficult, given these multiple possible origins as mentioned above (e.g., Donnelly et al., 2004; Escrig et al., 2004; Janney et al., 2005; Ulrich et al., 2012; Waters et al., 2011). Variations in La/Sm and Sm/Yb ratios indicate that the mafic rocks were derived by partial melting of lherzolite in the spinel stability field (Fig. 11). Fractional melting models show that the E-MORB- and P-MORB-type rocks could have been generated by ~5%–10% melting of depleted spinel-facies mantle, with varying amounts of OIB-like materials being involved (Fig. 7b and d).

6. Tectonic setting of the SNMZ: new insights from the Yunzhug ophiolite

To-date, two contrasting hypotheses have been proposed to explain the SNMZ. These involve the SNMZ being a long-distance southward nappe of the BNSZ ophiolite, or an independent ophiolitic belt within

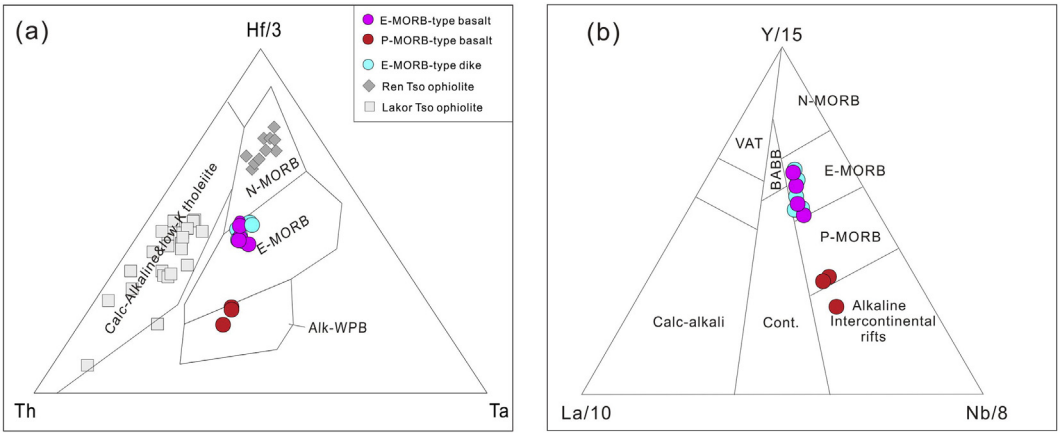

Fig. 8. (a) Hf–Th–Ta discrimination diagram (Wood, 1980) and (b) Y–La–Nb diagram (Cabanis and Lecolle, 1989). Data sources are the same as for Fig. 6.

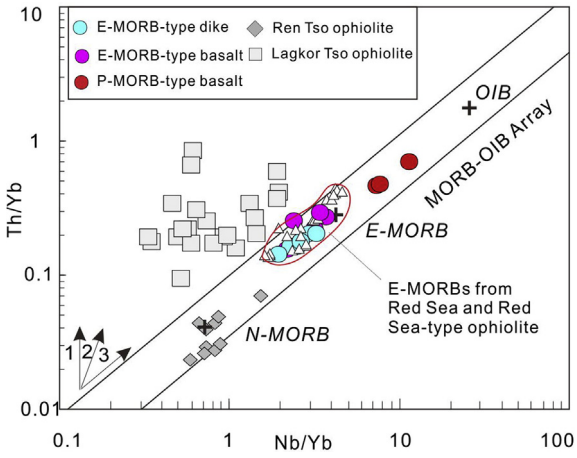

Fig. 9. Nb/Yb–Th/Yb discrimination diagram from Dilek and Furnes (2011) and Pearce (2014). Abbreviations: arrow 1 = subduction enrichment trend; arrow 2 = crustal contamination trend; arrow 3 = within-plate enrichment trend. Data for LakorTso ophiolite are from Yuan et al. (2015) and for RenTso ophiolite are from Zhong et al. (2015). Data for Jormua ophiolite are from Peltonen et al. (1996).

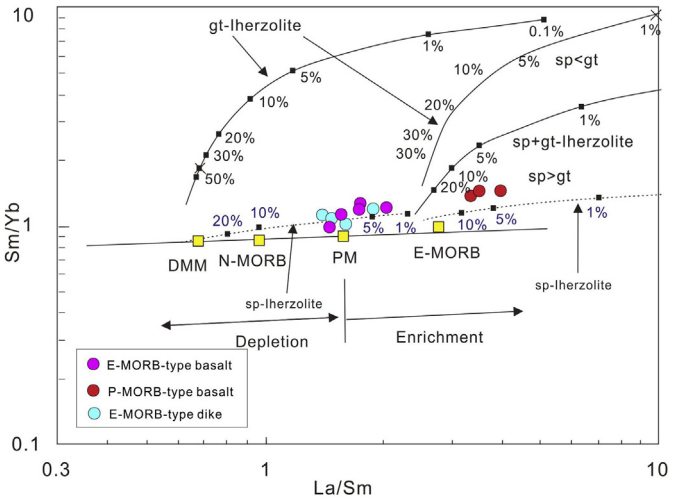

Fig. 11. Variations in La/Sm and Sm/Yb ratios in the Yunzhug mafic rocks, annotated with partial melting curves for garnet and spinel lherzolite mantle sources. (From Aldanmaz et al., 2000).

the Lhasa Terrane (Zhu et al., 2013, and references therein). These models are evaluated below in detail.

6.1. Southward nappe of the BNSZ ophiolite?

This model was originally proposed on the basis of similarities between the Yunzhug ophiolite and the Dongqiao ophiolite in the BNSZ (Fig. 1b) (Girardeau et al., 1985). However, our new zircon U–Pb dating indicates that the age of the Yunzhug ophiolite (~150 Ma) is very different from that of the Dongqiao ophiolite (~187.8 Ma; Liu et al., 2016). Moreover, the Bangong–Nujiang ophiolites are all spatially associated with Lower–Middle Jurassic Muggar Kangri Group flysch sediments (e.g., Kapp et al., 2003; Liu et al., 2016; Wang et al., 2016; K. J. Zhang et al., 2007; Zhu et al., 2013), whereas the Yunzhug, Ren Tso, and Namu Tso ophiolites are spatially associated with the Upper Jurassic–Lower Cretaceous Rila Formation and Paleozoic sedimentary rocks (Fig. 2) (Xu et al., 2014a). Thus, it is unlikely that only the Bangong–Nujiang ophiolites were affected by thrusting, given that the Muggar Kangri Group was not subjected to thrusting. Besides, the Yunzhug sheeted dike complex provides compelling structural evidence for horizontal extension during dike injection at a spreading ridge (Detrick et al., 1994; Metcalf and Shervais, 2008), and it has already been demonstrated that the ridge of the Bangong–Nujiang Ocean was subducted beneath the Qiangtang Terrane as early as ~157 Ma (Li et al., 2016). Therefore, the Yunzhug, Namu Tso, and Ren Tso ophiolites most likely represent an independent ophiolitic belt within the Lhasa Terrane.

6.2. Back-arc basin related to subduction of the Bangong–Nujiang oceanic crust?

Almost all previous studies that regarded the SNMZ as an independent ophiolitic belt proposed that it formed in a back-arc setting related to the southward subduction of the Bangong–Nujiang oceanic crust (Xu et al., 2014a; Yuan et al., 2015; Zhong et al., 2015; Zhu et al., 2011). However, this view was based mainly on studies of fluid-mobile elements or cumulate rocks. Although ophiolites can form in a variety of tectonic settings, in terms of geochemistry (Dilek and Furnes, 2011; Pearce, 2014), these different settings are: (1) influenced by subduction material with arc-like signatures, which normally fall in the field above the MORB array on a Nb/Yb–Th/Yb plot, such as back-arc and fore-arc basin rocks; (2) not influenced by subduction material, and lacking arc-signatures, such as rocks that form at mature MORs and in embryonic oceanic settings. The mafic rocks in the Yunzhug ophiolite are

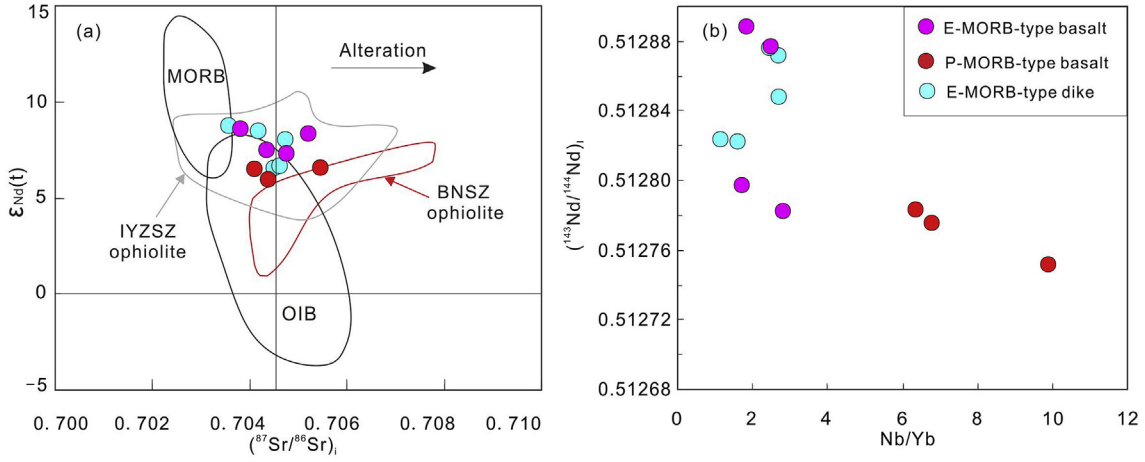

Fig. 10. Plots of $\varepsilon_{Nd}(t)$ versus $(^{87}Sr/^{86}Sr)_i$ and $(^{143}Nd/^{144}Nd)_i$ versus Nb/Yb for mafic rocks of the Yunzhug ophiolite. Data for mafic rocks from the BNSZ ophiolites are from Wang et al. (2016), and Liu et al. (2016). The field corresponding to MORB and OIB are modified from Zheng et al. (2017).

MORB-type rocks without any subduction signature (Fig. 7), which uniformly plot within the MORB array (Fig. 9), all of which are inconsistent with the back-arc model. In other tectonic discrimination diagrams, data for all our samples plot in non-arc fields (Fig. 8). The high Ti and low V contents of the rocks also indicate a source with a low oxygen fugacity, which differs from the source of back-arc basin basalts (Fig. 6b) (Shervais, 1982). Furthermore, no volcanic rocks, turbidites, or volcaniclastic rocks with ages older than the Yunzhug ophiolite are found in the northern Lhasa subterrane. This precludes the southward subduction of the Bangong–Nujiang oceanic crust beneath the Lhasa Terrane at a steep angle prior to the Jurassic, which would have been necessary for back-arc spreading (Sdrolias and Müller, 2006). All the points made above indicate that the back-arc basin model, driven by southward subduction of the Bangong–Nujiang oceanic crust, is not plausible.

6.3. Embryonic oceanic basin within the Lhasa Terrane?

Our new geochemical data for the mafic rocks in the Yunzhug area suggest a MOR-setting, which leads us to propose an alternative model for the genesis of the SNMZ. Globally, E-MORB-type oceanic crust either occurs at mature ocean ridges with slow spreading rates, ridges influenced by mantle plumes, or incipient spreading centers following continental break-up, such as the Red Sea (e.g., Dilek and Furnes, 2011; Pearce, 2014). Although our study indicates that the SNMZ was not the southward nappe of the BNSZ ophiolite, it is likely that they together constitute an intra-oceanic system of the Bangong–Nujiang Ocean, including possible fragments of oceanic plateau (e.g., Matte et al., 1996; K. J. Zhang et al., 2014). In this model, the northern Lhasa subterrane was an accretionary juvenile terrane during northward subduction of the Bangong–Nujiang oceanic crust, as indicated by the Hf isotopic values of zircons from igneous rocks (e.g., Zhu et al., 2011). Although we cannot rule out this possibility, we favor the hypothesis that the Yunzhug ophiolite formed in an embryonic ocean, for the following reasons. Firstly, the nearly symmetrically distributed Paleozoic strata on either side of the Yunzhug ophiolite (Fig. 2), and recent studies of Early Cretaceous magmatic rocks in the northern Lhasa subterrane, suggest that the northern Lhasa subterrane has a basement similar to that of the central Lhasa subterrane, but is now covered by Jurassic to Early Cretaceous sedimentary rocks (Sun et al., 2015). Secondly, the sediments of the Rila Formation comprise peridotite-bearing coarse-grained sandstone and conglomerate through to siliceous siltstone with radiolarite-bearing siliceous interbeds, pelsparite, calcirudite, and marble with black shale and siliceous layers, which represent Late Jurassic–Early Cretaceous bathyal–abyssal deposits (Qu et al., 2003; Volkmer et al., 2014; Zhang et al., 2011). In particular, the presence of black, organic-rich sediments suggests their formation in a restricted basin (e.g., Robertson, 2002). Moreover, the siliceous rocks interbedded with the pillow basalts of the Yunzhug ophiolite contain a large proportion of argillaceous components when compared with typical pelagic siliceous rocks, and these characteristics indicate formation near a continental margin, suggesting a narrow ocean basin located close to a continental margin (Xu et al., 2014b). Thirdly, the massive peridotites distributed on the western bank of Guomang Tso were derived from ancient subcontinental lithospheric mantle, as indicated by their Re–Os model ages (T_{RD} = 0.5–2.0 Ga, with a peak at 1.2 Ga; unpublished data of the authors), which is also typical of the ocean–continent transition zone (e.g., Rampone and Piccardo, 2000; Shi et al., 2012). Fourthly, paleomagnetic research has reported insignificant latitudinal convergence (~3.2°) during the Early Cretaceous within the Lhasa Terrane (Li et al., 2015, and references therein). All the above arguments support the concept that the oceanic realm was narrow. This model can account for the arc-like signatures of the Middle Jurassic mafic rocks from the Lagkor Tso and Shiquanhe ophiolites in the same ophiolitic belt by contamination from continental lithosphere prior to continental break-up and sea-floor spreading (Figs. 6–9) (e.g., Dilek and Furnes, 2011; Pearce, 2014; Robertson, 2002). In this regard, the SNMZ was also not the southward-directed nappe of the Bangong–Nujiang ophiolites because the embryonic oceanic crust was ~278 Ma in age (Chen et al., 2017).

6.4. Geodynamic implications

Northwards subduction of the Neo-Tethys oceanic crust in conjunction with the southwards subduction of the Bangong–Nujiang oceanic crust, or northwards subduction of the Neo-Tethys oceanic crust on its own have been commonly invoked to explain the Jurassic tectonomagmatic evolution of the Lhasa Terrane (e.g., Zhu et al., 2009). These previous models are evaluated in more detail below. The first model states that the Bangong–Nujiang oceanic crust started to be subducted beneath the Lhasa Terrane during the late Permian–Early Triassic (Chen et al., 2015), and that the Neo-Tethys Ocean and Yunzhug Ocean were successively opened as back-arc basins during the Late Triassic to Middle Jurassic and Early Cretaceous, respectively (e.g., Zhu et al., 2009, 2011). Although additional revised models interpreting the SNMZ as a Jurassic back-arc basin have been proposed (e.g., Pan et al., 2012; Xu et al., 2014a; Zhong et al., 2015), these are all problematic given that the SNMZ formed in a MOR-setting rather than in a back-arc basin setting. Thus, our evidence from the Yunzhug ophiolite provides evidence that argues against southward subduction of the Bangong–Nujiang oceanic crust. This is consistent with the Nd isotopic signatures of (K.J. Zhang et al., 2007) and detrital zircons in (Zeng et al., 2016 and reference therein) Middle Jurassic sedimentary rocks of the northern Lhasa subterrane, which indicate formation in a passive margin environment.

The second model proposes that subduction of the Neo-Tethys oceanic crust started in the Late Triassic–Early Jurassic (e.g., Ji et al., 2009; Zhang et al., 2012; Ma et al., 2017), and that this became flat subduction during the Middle Jurassic to Early Cretaceous (Kapp et al., 2003, 2007; Zhang et al., 2004, 2011, 2012). In this model, the Bangong–Nujiang oceanic crust was never subducted southwards. However, the central and northern Lhasa subterranes were in a compressional environment, and a southward-nappe model is used to explain the genesis of the SNMZ. This model is also inconsistent with our studies on the Yunzhug ophiolite.

In summary, existing models do not adequately explain the formation of the SNMZ within the Lhasa Terrane. Our preferred model is that the SNMZ was formed in an embryonic ocean after continental break-up of the Lhasa Terrane, which was probably driven by a mantle plume or far-field plate tectonic forces such as the relaxation of convergent-plate-induced stress (e.g., Merle, 2011; Rosenbaum et al., 2008). Given that there is no evidence for Jurassic mantle plume activity within the Lhasa Terrane, the break-up of the Lhasa Terrane continental lithosphere was probably related to the relaxation of convergent stress or pull-apart effects due to the northward subduction of the Neo-Tethys and Bangong–Nujiang oceanic crust. Although the mechanism that caused continental break-up of the Lhasa Terrane remains unclear, further investigation would provide important new insights into the Jurassic tectonic evolution of the Lhasa Terrane.

7. Conclusions

(1) The Yunzhug ophiolite within the Lhasa Terrane formed at 150.5 ± 3.6 Ma, based on zircon U–Pb dating of a gabbroic sample from a well-developed sheeted dike complex.
(2) The Yunzhug mafic rocks are MORB-type in composition, without any influence of slab-released materials, which suggests they formed in a MOR-setting rather than a back-arc basin setting as has been conventionally thought.
(3) The Yunzhug ophiolite is part of an independent ophiolitic belt that formed within an embryonic ocean in the Lhasa Terrane, and thus is inconsistent with southward subduction of the Bangong–Nujiang oceanic crust.

Acknowledgments

We thank Nelson Eby (Editor), Dr. Chen Sheng-Sheng, and an anonymous reviewer for their constructive comments that helped us to improve the quality of this manuscript. We also thank Alan Baxter and Solomon Buckman for thoughtful advice on an earlier draft. This research was supported by the following funding agencies: National Key Research and Development Project of China (project 2016YFC0600305, 2016YFC0600304), the Major State Basic Research Program of the People's Republic of China (2015CB452602), the Natural Science Foundation of China (41463001, 41573024, 41603033, 41730427, 41773026), the Fundamental Research Funds for the Central Universities (53200759031) and the Support Program of National Postdoctor Program for Innovative Talents (BX201700213).

Appendix A. Supplementary data

Supplementary data to this article can be found online at https://doi.org/10.1016/j.lithos.2017.11.025.

References

Aldanmaz, E., Pearce, J.A., Thirlwall, M.F., Mitchell, J.G., 2000. Petrogenetic evolution of late Cenozoic, post-collision volcanism in western Anatolia, Turkey. Journal of Volcanology and Geothermal Research 102, 67–95.

Baxter, A.T., Aitchison, J.C., Zyabrev, S.V., 2009. Radiolarian age constraints on Mesotethyan ocean evolution, and their implications for development of the Bangong-Nujiang suture, Tibet. Journal of the Geological Society 166 (4), 689–694.

Cabanis, B., Lecolle, M., 1989. Le diagram La/10-Y/15-Nb/8: un outil pour la discrimination des series volcaniques et la mise en evidence des processus de melange etou de contamination crustale. Comptes Rendus de l'Academie des Sciences Serie II 309, 2023–2029.

Chen, S.S., Shi, R.D., Zou, H.B., Huang, Q.S., Liu, D.L., Gong, X.H., Yi, G.D., Wu, K., 2015. Late Triassic island-arc–back-arc basin development along the Bangong–Nujiang suture zone (central Tibet): geological, geochemical and chronological evidence from volcanic rocks. Lithos 230, 30–45.

Chen, S.S., Shi, R.D., Fan, W.M., Gong, X.H., Wu, K., 2017. Early Permian mafic dikes in the Nagqu area, central Tibet, China, associated with embryonic oceanic crust of the Meso-Tethys Ocean. Journal of Geophysical Research - Solid Earth. https://doi.org/10.1002/2016JB013693.

Chung, S.L., Chu, M.F., Zhang, Y., Xie, Y., Lo, C.H., Lee, H.Y., Lan, C.Y., Li, X., Zhang, Q., Wang, Y., 2005. Tibetan tectonic evolution inferred from spatial and temporal variations in post-collisional magmatism. Earth-Science Reviews 68 (3), 173–196.

Corfu, F., Hanchar, J.M., Hoskin, P., Kinny, P., 2003. Atlas of zircon textures. Reviews in Mineralogy and Geochemistry 16, 469–500.

Coulon, C., Maluski, H., Bollinger, C., Wang, S., 1986. Mesozoic and Cenozoic volcanic rocks from central and southern Tibet: 39Ar–40Ar dating, petrological characteristics and geodynamical significance. Earth and Planetary Science Letters 79 (3), 281–302.

Detrick, R., Collins, J., Stephen, R., Swift, S., 1994. In situ evidence for the nature of the seismic layer 2/3 boundary in oceanic crust. Nature 370 (6487), 288–290.

Dilek, Y., Furnes, H., 2011. Ophiolite genesis and global tectonics: geochemical and tectonic fingerprinting of ancient oceanic lithosphere. Geological Society of America Bulletin 123 (3–4), 387–411.

Donnelly, K.E., Goldstein, S.L., Langmuir, C.H., Spiegelman, M., 2004. Origin of enriched ocean ridge basalts and implications for mantle dynamics. Earth and Planetary Science Letters 226 (3–4), 347–366.

Escrig, S., Capmas, F., Dupré, B., Allègre, C.J., 2004. Osmium isotopic constraints on the nature of the DUPAL anomaly from Indian mic-ocean-ridge basalts. Nature 431, 59–63.

Girardeau, J., Marcoux, J., Fourcade, E., Bassoullet, J.P., Youking, T., 1985. Xainxa ultramafic rocks, central Tibet, China: tectonic environment and geodynamic significance. Geology 13 (5), 330–333.

Goldstein, S.L., O'Nions, R.K., Hamilton, P.J., 1984. A Sm-Nd isotopic study of atmospheric dusts and particulates from major river systems. Earth and Planetary Science Letters 70, 221–236.

Grimes, C.B., John, B.E., Kelemen, P.B., Mazdab, F.K., Wooden, J.L., Cheadle, M.J., Hanghøj, K., Schwartz, J.J., 2007. Trace element chemistry of zircons from oceanic crust: a method for distinguishing detrital zircon provenance. Geology 35 (7), 643–646.

Grimes, C.B., Wooden, J.L., Cheadle, M.J., John, B.E., 2015. "Fingerprinting" tectono-magmatic provenance using trace elements in igneous zircon. Contribution to Mineralogy and Petrology 158, 757–783.

Haase, K.M., Mühe, R., Stoffers, P., 2000. Magmatism during extension of the lithosphere: geochemical constraints from lavas of the Shaban Deep, northern Red Sea. Chemical Geology 166 (3), 225–239.

He, Z.H., Yang, D.M., Wang, T.W., 2006. Age, geochemistry and its tectonic significance of Kaimeng ophiolites in Jiali fault belt, Tibet. Acta Petrologica Sinica 22 (3), 653–660 (in Chinese with English abstract).

Hoskin, P., 2000. Patterns of chaos: fractal statistics and the oscillatory chemistry of zircon. Geochimica et Cosmochimica Acta 64, 1905–1923.

Hoskin, P., Black, L.P., 2000. Metamorphic zircon formation by solid-state recrystallization of protolith igneous zircon. Journal of Metamorphic Geology 18, 423–439.

Janney, P.E., Le Roex, A.P., Carlson, R.W., 2005. Hafnium isotope and trace element constraints on the nature of mantle heterogeneity beneath the Central Southwest Indian Ridge (13°E to 47°E). Journal of Petrology 46, 2427–2464.

Ji, W.Q., Wu, F.Y., Chung, S.L., Li, J.X., Liu, C.Z., 2009. Zircon U–Pb geochronology and Hf isotopic constraints on petrogenesis of the Gangdese batholith, southern Tibet. Chemical Geology 262 (3), 229–245.

Ji, W.Q., Wu, F.Y., Chung, S.L., Wang, X.C., Liu, C.Z., Li, Q.L., Liu, Z.C., Liu, X.C., Wang, J.G., 2016. Eocene Neo-Tethyan slab breakoff constrained by 45 Ma oceanic island basalt–type magmatism in southern Tibet. Geology 44 (4), 283–286.

Kang, Z., Xu, J., Wilde, S.A., Feng, Z., Chen, J., Wang, B., Fu, W., Pan, H., 2014. Geochronology and geochemistry of the Sangri group volcanic rocks, southern Lhasa Terrane: implications for the early subduction history of the Neo-Tethys and Gangdese magmatic arc. Lithos 200, 157–168.

Kapp, P., Murphy, M.A., Yin, A., Harrison, T.M., Ding, L., Guo, J., 2003. Mesozoic and Cenozoic tectonic evolution of the Shiquanhe area of western Tibet. Tectonics 22 (4).

Kapp, P., DeCelles, P.G., Gehrels, G.E., Heizler, M., Ding, L., 2007. Geological records of the Lhasa-Qiangtang and Indo-Asian collisions in the Nima area of central Tibet. Geological Society of America Bulletin 119 (7–8), 917–933.

Leat, P.T., Livermore, R.A., Millar, I.L., Pearce, J.A., 2000. Magma supply in back-arc spreading centre segment E2, East Scotia Ridge. Journal of Petrology 41 (6), 845–866.

Li, Z., Ding, L., Song, P., Fu, J., Yue, Y., 2015. Paleomagnetic constraints on the paleolatitude of the Lhasa block during the Early Cretaceous: implications for the onset of India–Asia collision and latitudinal shortening estimates across Tibet and stable Asia. Gondwana Research. https://doi.org/10.1016/j.gr.2015.05.013.

Li, S.M., Zhu, D.C., Wang, Q., Zhao, Z.D., Zhang, L.L., Liu, S.A., Chang, Q.S., Lu, Y.H., Dai, J.G., Zheng, Y.C., 2016. Slab-derived adakites and subslab asthenosphere-derived OIB-type rocks at 156 ± 2 Ma from the north of Gerze, central Tibet: records of the Bangong–Nujiang oceanic ridge subduction during the Late Jurassic. Lithos 262, 456–469.

Liu, T., Zhai, Q.G., Wang, J., Bao, P.S., Qiangba, Z., Tang, S.H., Tang, Y., 2016. Tectonic significance of the Dongqiao ophiolite in the north-central Tibetan plateau: evidence from zircon dating, petrological, geochemical and Sr–Nd–Hf isotopic characterization. Journal of Asian Earth Sciences 116, 139–154.

Li, X., Mo, X., Scheltens, M., Guan, Q., 2017. Mineral chemistry and crystallization conditions of the Late Cretaceous Mamba pluton from the eastern Gangdese, Southern Tibetan Plateau. Journal of Earth Science 27, 545–570.

Ma, X., Xu, Z., Chen, X., Meert, J.G., He, Z., Liang, F., Meng, Y., Ma, S., 2017. The origin and tectonic significance of the volcanic rocks of the Yeba Formation in the Gangdese magmatic belt. South Tibet. Journal of Earth Science 28, 265–282.

Matte, P., Tapponnier, P., Arnaud, N., Bourjot, L., Avouac, J.P., Vidal, P., Liu, Q., Pan, Y.S., Wang, Y., 1996. Tectonics of Western Tibet, between the Tarim and the Indus. Earth and Planetary Science Letters 142, 311–330.

Merle, O., 2011. A simple continental rift classification. Tectonophysics 513 (1), 88–95.

Metcalf, R.V., Shervais, J.W., 2008. Suprasubduction-zone ophiolites: is there really an ophiolite conundrum? Geological Society of America Special Papers 438, 191–222.

Pan, G., Wang, L.Q., Li, R., Yuan, S.H., Ji, W.H., Yin, F.G., Zhang, W., Wang, B.D., 2012. Tectonic evolution of the Qinghai-Tibet plateau. Journal of Asian Earth Sciences 53, 3–14.

Pearce, J.A., 2014. Immobile element fingerprinting of ophiolites. Elements 10 (2), 101–108.

Peltonen, P., Kontinen, A., Huhma, H., 1996. Petrology and geochemistry of metabasalts from the 1.95 Ga Jormua ophiolite, northeastern Finland. Journal of Petrology 37 (6), 1359–1383.

Petrini, R., Joron, J.L., Ottonello, G., Bonatti, E., Seyler, M., 1988. Basaltic dykes from Zabargad Island, Red Sea: petrology and geochemistry. Tectonophysics 150 (1), 229–248.

Qu, Y.G., Zhang, S.Q., Zheng, C.Z., Wang, Y.S., Lu, P., Wang, H.S., Li, X.B., Li, Q.W., 2003. The Late Jurassic-Early Cretaceous Rila formation Suoer clastic rocks and characteristics of biotas in the Yunzhug ophiolitic belt, northern Tibet. Geological Bulletin of China 22, 11–12 (in Chinese with English abstract).

Rampone, E., Piccardo, G.B., 2000. The ophiolite-oceanic lithosphere analogue: new insights from the Northern Apennines (Italy). Special Papers-Geological Society of America 21–34.

Rehka, M., Hofmann, A.W., 1997. Recycled ocean crust and sediment in Indian Ocean MORB. Earth and Planetary Science Letters 147 (1), 93–106.

Robertson, A.H., 2002. Overview of the genesis and emplacement of Mesozoic ophiolites in the Eastern Mediterranean Tethyan region. Lithos 65 (1), 1–67.

Rosenbaum, G., Weinberg, R.F., Regenauer-Lieb, K., 2008. The geodynamics of lithospheric extension. Tectonophysics 458 (1), 1–8.

Saccani, E., Azimzadeh, Z., Dilek, Y., Jahangiri, A., 2013. Geochronology and petrology of the Early Carboniferous Misho Mafic Complex (NW Iran), and implications for the melt evolution of Paleo-Tethyan rifting in Western Cimmeria. Lithos 162–163, 264–278.

Sdrolias, M., Müller, R.D., 2006. Controls on back-arc basin formation. Geochemistry, Geophysics, Geosystems 7 (4), Q04016.

Shervais, J.W., 1982. Ti–V plots and the petrogenesis of modern and ophiolitic lavas. Earth and Planetary Science Letters 59 (1), 101–118.

Shi, R., Griffin, W.L., O'Reilly, S.Y., Huang, Q., Zhang, X., Liu, D., Zhi, X.C., Xiq, Q.X., Ding, L., 2012. Melt/mantle mixing produces podiform chromite deposits in ophiolites: implications of Re–Os systematics in the Dongqiao Neo-tethyan ophiolite, northern Tibet. Gondwana Research 21 (1), 194–206.

Sun, S.S., McDonough, W.F., 1989. Chemical and isotopic systematics of oceanic basalts: implications for mantle composition and processes. Geological Society, London, Special Publications 42 (1), 313–345.

Sun, S.J., Sun, W.D., Zhang, L.P., Zhang, R.Q., Li, C.Y., Zhang, H., Hu, Y.B., Zhang, Z.R., 2015. Zircon U–Pb ages and geochemical characteristics of granitoids in Nagqu area, Tibet. Lithos 231, 92–102.
Ulrich, M., Hémond, C., Nonnotte, P., Jochum, K.P., 2012. OIB/seamount recycling as a possible process for E-MORB genesis. Geochemistry, Geophysics, Geosystems 13 (1).
Volkmer, J.E., Kapp, P., Horton, B.K., Gehrels, G.E., Minervini, J.M., Ding, L., 2014. Northern Lhasa thrust belt of central Tibet: evidence of Cretaceous–early Cenozoic shortening within a passive roof thrust system? Geological Society of America Special Papers 507, 59–70.
Wang, Y.S., Qu, Y.G., Wang, Z.H., Zheng, C.Z., Xie, Y.H., Sun, Z.G., Zhang, N.K., 2005. Discovery of the Yunzhug sheeted dike swarm in northern Tibet, China–evidence for seafloor spreading. Geological Bulletin of China 24 (12), 1150–1156 (in Chinese with English abstract).
Wang, W.L., Aitchison, J.C., Lo, C.H., Zeng, Q.G., 2008. Geochemistry and geochronology of the amphibolite blocks in ophiolitic mélanges along Bangong-Nujiang suture, central Tibet. Journal of Asian Earth Sciences 33 (1), 122–138.
Wang, B.D., Wang, L.Q., Chung, S.L., Chen, J.L., Yin, F.G., Liu, H., Li, X.B., Chen, L.K., 2016. Evolution of the Bangong–Nujiang Tethyan ocean: insights from the geochronology and geochemistry of mafic rocks within ophiolites. Lithos 53, 18–33.
Waters, C.L., Sims, K.W.W., Perfit, M.R., Blichert-Toft, J., Blusztajn, J., 2011. Perspective on the genesis of E-MORB from chemical and isotopic heterogeneity at 9–10 N East Pacific rise. Journal of Petrology 52 (3), 565–602.
Winchester, J.A., Floyd, P.A., 1977. Geochemical discrimination of different magma series and their differentiation products using immobile elements. Chemical Geology 20, 325–343.
Wood, D.A., 1980. The application of a Th Hf Ta diagram to problems of tectonomagmatic classification and to establishing the nature of crustal contamination of basaltic lavas of the British Tertiary Volcanic Province. Earth and Planetary Science Letters 50 (1), 11–30.
Wu, Y., Li, C., Xu, M., Xie, C., Wang, M., 2017. Zircon U-Pb age, geochemical data: Constraints on the origin and tectonic evolution of the metamafic rocks from Longmuco-Shuanghu-Lancang suture zone, Tibet. Journal of Earth Science 28, 422–432.
Xu, M.J., Li, C., Zhang, X.Z., Wu, Y.W., 2014a. Nature and evolution of the Neo-Tethys in central Tibet: synthesis of ophiolitic petrology, geochemistry, and geochronology. International Geology Review 56 (9), 1072–1096.
Xu, M.J., Li, C., Wu, Y.W., Xie, C.M., 2014b. Geochemical characteristics and sedimentary environments of siliceous rocks in Guomang-co ophiolitic mélange of Tibet. Geological Bulletin of China 33 (7), 1061–1066 (in Chinese with English abstract).
Yin, A., Harrison, T.M., 2000. Geologic evolution of the Himalayan-Tibetan orogen. Annual Review of Earth and Planetary Sciences 28 (1), 211–280.
Yuan, H.L., Gao, S., Liu, X.M., Li, H.M., Günther, D., Wu, F.Y., 2004. Accurate U-Pb age and trace element determinations of zircon by laser ablation–inductively coupled plasma mass spectrometry. Geostandards and Geoanalytical Research 28 (3), 353–370.
Yuan, H.-L., Gao, S., Dai, M.-N., Zong, C.-L., Günther, D., Fontaine, G.H., Liu, X.-M., Diwu, C., 2008. Simultaneous determinations of U–Pb age, Hf isotopes and trace element compositions of zircon by excimer laser-ablation quadrupole and multiple-collector ICP-MS. Chemical Geology 237, 100–118.
Yuan, Y.J., Yin, Z.X., Liu, W.L., Huang, Q.T., Li, J.F., Liu, H.F., Wan, Z.F., Cai, Z., Xia, B., 2015. Tectonic evolution of the Meso-Tethys in the western segment of Bangonghu-Nujiang suture zone: insights from geochemistry and geochronology of the Lagkor Tso ophiolite. Acta Geologica Sinica (English Edition) 89 (2), 369–388.
Zeng, Y.C., Chen, J.L., Xu, J.F., Wang, B.D., Huang, F., 2016. Sediment melting during subduction initiation: geochronological and geochemical evidence from the Darutso high-Mg andesites within ophiolite melange, central Tibet. Geochemistry, Geophysics, Geosystems 17 (12), 4859–4877.
Zeng, Y.C., Xu, J.F., Chen, J.L., Wang, B.D., Huang, F., Yu, H.X., Chen, X.F., Zhao, P.P., 2017. Breakup of eastern Gondwana as inferred from the Lower Cretaceous Charong Dolerites in the central Tethyan Himalaya, southern Tibet. Palaeogeography, Palaeoclimatology, Palaeoecology. https://doi.org/10.1016/j.palaeo.2017.10.010.
Zhang, K.J., Xia, B.B., Wang, G., Li, Y.T., Ye, H.F., 2004. Early Cretaceous stratigraphy, depositional environments, sandstone provenance, and tectonic setting of central Tibet, western China. Geological Society of America Bulletin 116 (9–10), 1202–1222.
Zhang, K.J., Zhang, Y.X., Li, B., Zhong, L.F., 2007. Nd isotopes of siliciclastic rocks from Tibet, western China: constraints on provenance and pre-Cenozoic tectonic evolution. Earth and Planetary Science Letters 256 (3), 604–616.
Zhang, Y.X., Zhang, K.J., Li, B., Wang, Y., Wei, Q., Tang, X., 2007. Zircon SHRIMP U–Pb geochronology and petrogenesis of the plagiogranites from the Lagkor Lake ophiolite, Gerze, Tibet, China. Chinese Science Bulletin 52 (5), 651–659.
Zhang, Q.H., Ding, L., Cai, F.L., Xu, X.X., Zhang, L.Y., Xu, Q., Willems, H., 2011. Early Cretaceous Gangdese retroarc foreland basin evolution in the Selin Co basin, central Tibet: evidence from sedimeNeo-Tethys Oceanlogy and detrital zircon geochronology. Geological Society, London, Special Publications 353 (1), 27–44.
Zhang, K.J., Zhang, Y.X., Tang, X.C., Xia, B., 2012. Late Mesozoic tectonic evolution and growth of the Tibetan plateau prior to the Indo-Asian collision. Earth-Science Reviews 114 (3), 236–249.
Zhang, K.J., Xia, B., Zhang, Y.X., Liu, W.L., Zeng, L., Li, J.F., Xu, L.F., 2014. Central Tibetan Meso-Tethyan oceanic plateau. Lithos 210, 278–288.
Zhang, Z.M., Dong, X., Santosh, M., Zhao, G.C., 2014. Metamorphism and tectonic evolution of the Lhasa terrane, Central Tibet. Gondwana Research 25 (1), 170–189.
Zheng, Y.Y., Xu, R.K., Ma, G.T., Gao, S.B., Zhang, G.Y., Ma, X.M., 2006. Ages of generation and subduction of Shiquan river ophiolite: restriction from SHRIMP zircon dating. Acta Petrologica Sinica 22 (4), 895–904 (in Chinese with English abstract).
Zheng, H., Huang, Q., Kapsiotis, A., Xia, B., Yin, Z., Zhong, Y., Lu, Y., Shi, X., 2017. Early Cretaceous ophiolites of the Yarlung Zangbo Suture Zone: insights from dolerites and peridotites from the Baer upper mantle suite, SW Tibet (China). International Geology Review 59 (11), 1471–1489.
Zhong, Y., Xia, B., Liu, W.L., Yin, Z.X., Hu, X.C., Huang, W., 2015. Geochronology, petrogenesis and tectonic implications of the Jurassic Namco–Renco ophiolites, Tibet. International Geology Review 57, 508–528.
Zhu, Z., 2004. The Geochemical Characteristics and Tectonic Setting About Ophiolite in Yunzhug-Namucuo, Tibet Plateau. (M.S. Thesis). Jilin University, Jilin, China (in Chinese with English abstract).
Zhu, D.C., Mo, X.X., Niu, Y., Zhao, Z.D., Wang, L.Q., Liu, Y.S., Wu, F.Y., 2009. Geochemical investigation of Early Cretaceous igneous rocks along an east–west traverse throughout the central Lhasa Terrane, Tibet. Chemical Geology 268 (3), 298–312.
Zhu, D.C., Zhao, Z.D., Niu, Y., Mo, X.X., Chung, S.L., Hou, Z.Q., Wang, L.Q., Wu, F.Y., 2011. The Lhasa Terrane: record of a microcontinent and its histories of drift and growth. Earth and Planetary Science Letters 301 (1), 241–255.
Zhu, D.C., Zhao, Z.D., Niu, Y., Dilek, Y., Hou, Z.Q., Mo, X.X., 2013. The origin and pre-Cenozoic evolution of the Tibetan Plateau. Gondwana Research 23 (4), 1429–1454.